Earthquake Engineering, Tenth World Conference © 1992 Balkema, Rotterdam. ISBN 90 5410 060 5

Interpretation of high pressure pipeline damage by liquefaction-induced ground movements

F. Miura
Yamaguchi University, Ube, Japan

T. D. O'Rourke
Cornell University, Ithaca, USA

M. Hamada
Tokai University, Shimizu, Japan

ABSTRACT: During the 1971 San Fernando earthquake, large ground deformations occurred at the Joseph Johnson Filtration Plant along the west side of the Upper Van Norman Reservoir. Recent analyses of aerial photographs taken before and after the earthquake have provided a comprehensive view of lateral and vertical ground movements at the site. Most pipelines in the utility corridor at the site were not damaged, but some pipelines were damaged by the ground movements. The object of this study is to show by numerical analyses why some of the pipelines were damaged while others were not. The analyses showed that for in-situ stress and frictional resistance pertaining to medium dense sand, almost the same magnitudes of stress as that of the yield stress were estimated at a location where tensile failure occurred for Grade-B steel pipelines. But lower stress levels were estimated for x-52 steel pipelines, which sustained the ground movements.

1 AIR PHOTO AND OPTICAL SURVEY MEASUREMENTS

Photogrammetric analyses were performed on high quality air photographs taken before and after the 1971 San Fernando earthquake for the west side of the Upper Van Norman Reservoir area (O'Rourke et al. 1989), where large ground displacements occurred during the earthquake. The interpretation process has been discussed in several publications

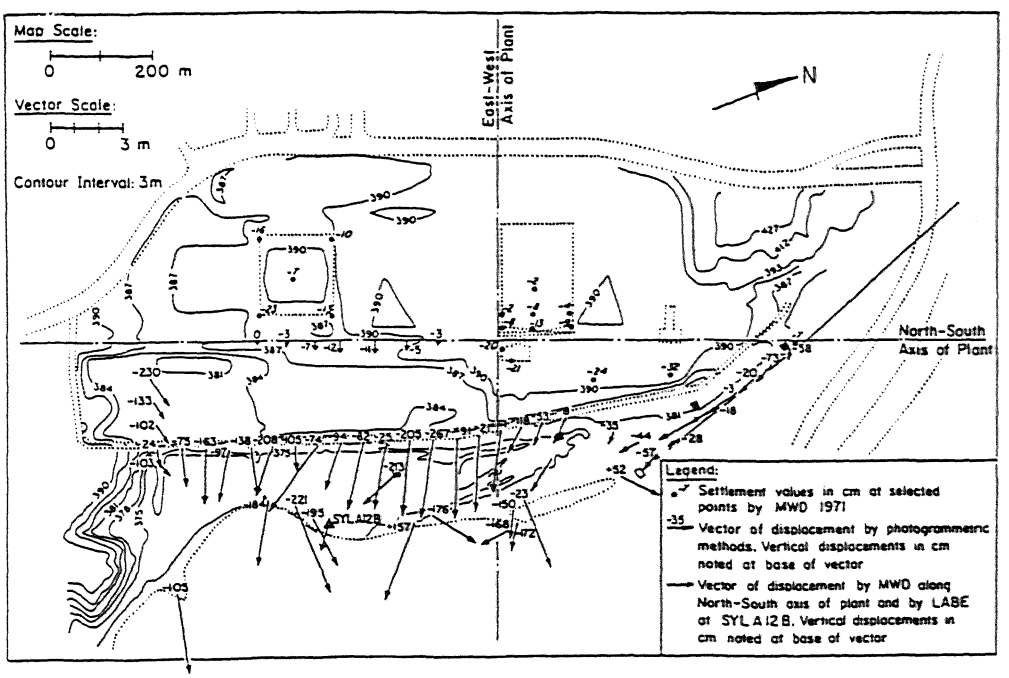

Figure 1. Displacements determined from air photo analyses and optical surveys.

(e.g. Hamada et al. 1985). The results of these analyses are shown in Figure 1 as vectors of horizontal movement and measurements of settlement and heave. Measurement accuracy is approximately 10 to 20 mm for lateral movement and settlement. Optical survey measurements performed by the Metropolitan Water District of Southern California (MWD) are also shown at various locations. For example, lateral offsets surveyed along the north-south plant axis and settlements at several key structures are included in the figure.

The air photo analyses show lateral ground movements along the utility corridor, typically 2 to 3 m, in an easterly direction toward the reservoir. At the eastern terminus of the Outlet Conduit, air photo measurements show lateral soil movements of 1.3 to 2.2 m, which agree reasonably well with the total cumulative movement measured on the ground at this location.

2 PIPELINE DAMAGE AT THE UPPER VAN NORMAN RESERVOIR

Figure 2 shows a plan view of the area west of the Upper Van Norman Reservoir on which are superimposed ground ruptures associated with liquefaction-induced ground failures in this locality. The locations of pipeline damage were determined from repair records provided through the courtesy of the Los Angeles Department of Water and Power (LADWP) and the Getty Oil Company. The information in the repair records was supplemented by discussions with utility personnel. The locations of pipeline repairs are designated by solid triangles in the figure. Table 1 summarizes information about the pipelines and includes dimensions, installation date, composition, joint type, coating, depth of soil cover, and nominal operating pressure at the time of the earthquake. The outside diameter (O.D.) and wall thickness for each pipe are listed in the column headed dimension. Each pipeline is numbered for the purpose of referencing and corresponds to the numbers used in the Typical Section in Figure 2. In general, the pipelines were buried in medium dense and silty sands above the water table. Transmission pipelines for natural gas, liquid fuel, and water were involved, representing different dimensions, joint design, operating pressures, welding practices, and age. Pipelines operated by the Los Angeles Department of Water and Power and the Southern California Gas Company are prefaced by DWP and SCG, respectively.

Most pipelines in the utility corridor were not damaged, including the three lines operated by the Southern California Gas Company and one operated by the Mobil Oil Corporation (pipelines 6a, 6b, 7, and 9 in Table 1). Some gas pipelines were cut and rewelded after the earthquake, principally to relieve residual stresses and make adjustment for deformations caused by the ground movements. Pipeline 8, operated by the Getty

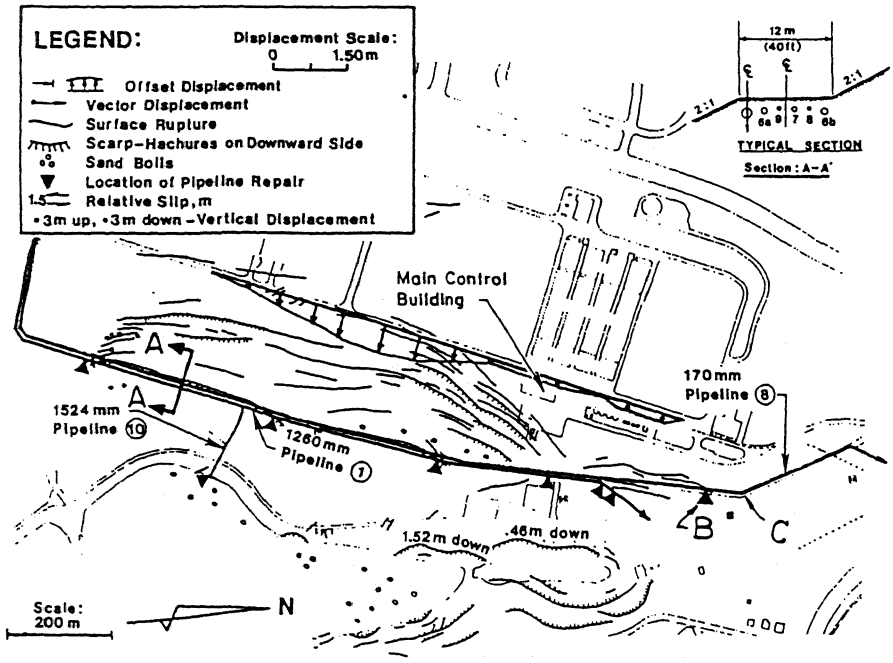

Figure 2. Locations of pipeline repairs, west side of the Upper Van Norman Reservoir.

Table 1. Information summary for pipelines affected by ground movements.

Number	Pipeline	Dimensions	Installation Date	Composition	Joints	Coating	Depth of Cover	Operating Pressure
1	DWP Granada Trunk Line	1260mm O.D.; 6.4mm wall thickness	1967	Steel, ASTM A-283 Grade C	Arc welded slip joints on 9m centers	Cement, 25.4mm thick	1.0m	0.7-1.4MPa
6a, 6b	SCG Lines 3000 & 3003	760mm O.D.; 9.5mm wall thickness	1966	Steel, X-52 Grade	Arc welded girth joints on 12m centers	Asphalt, fiberglass, asbestos felt	1.0-1.2m	1.4-3.2MPa
7	SCG Line 120	560mm O.D.; 7.2mm wall thickness	1966	Steel, X-52 Grade	Arc welded girth joints on 12m centers	Asphalt, fiberglas and asbestos felt	1.0-1.2m	1.4MPa
8	Getty Oil Company Line	170mm O.D.; 7.2 mm wall thickness	1966	Steel, API Grade B	Arc welded girth joints on 12m centers	Coal tar enamel & fiberglas	1.0-1.2m	0.7-1.0MPa
9	Mobil Oil Corporation Line	400mm O.D.; 7.9mm wall thickness	1966 1969	Steel, X-52 Grade	Arc welded girth joints on 12m centers	Coal tar enamel & fiberglas	1.0-1.2m	No internal pressure at time of earthquake
10	DWP Plant Connection	1524mm O.D.; 9.5mm wall thickness	1970	Steel, ASTM A-283 Grade C	Arc welded slip joints on 9m centers	0.6m thick reinforced concrete encasement	2.0m	No internal pressure at time of earthquake

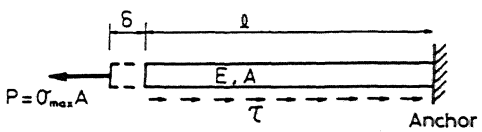

Figure 3. A model of a pipe for numerical analyses.

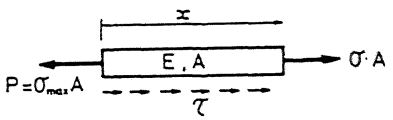

Figure 4. The equeliburium condition.

Oil Company, failed in tension across a weld at the northern boundary of the landslide area (Point B in Figure 2). The analyses for pipeline 8 are discussed in the following chapter. Detailed discussion of the damage at other points is given by O'Rourke et al. (1990).

3 NUMERICAL ANALYSES

In order to interpret the reason why some of the pipelines were damaged at point B in Figure 2, while others were not damaged, numerical analyses were performed to evaluate the response of the pipelines to ground movements. The pipelines were assumed to be anchored at location C in Figure 2, where the pipelines bend to the northwest. Based on this assumption, the model shown in Figure 3 was empoyed to estimate the maximum tensile stress, σ_{max}, in the pipelines at location B in Figure 2, where tensile failure was observed for pipeline 8. The magnitude of δ, which is the elongation of the pipe at the length, ℓ, was obtained by assuming that the pipelines south of location C were deformed in accordance with the ground displacements shown in Figure 1.

3.1 The relationship between δ and σ_{max}

The equilibrium condition of part of a pipeline of which length is x is given by (see Figure 4);

$$\sigma = \sigma_{max} - \frac{\tau}{A} x \qquad (1)$$

where, σ = stress at x, σ_{max} = the maximum stress at the end of the pipe, τ = shearing resistance along the pipe per unit length, A = area of cross-section of the pipe.

The shearing resistance, τ, is assumed to be a function of the unit weight of soil, γ, the coefficient of earth pressure at rest, Ko, the depth of the pipe below the ground surface, H, the outer diameter of the pipe, D, and the friction angle between the pipe and soil, ϕ, and is given by;

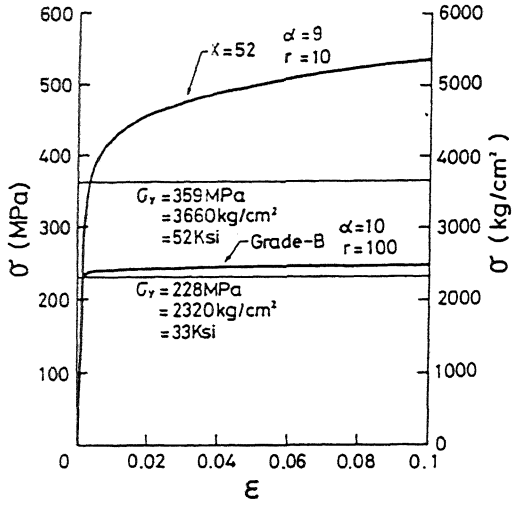

Figure 5. The stress-strain curves for analyzed pipes.

$$\tau = \frac{1+K_o}{2}\gamma H \tan\phi \, \pi D \qquad (2)$$

The relationship between stress and strain induced in the pipe is expressed by Equation (3) by assuming the Ramberg-Osgood stress-strain relationship;

$$\varepsilon = \frac{\sigma}{E}\left\{1 + \frac{\alpha}{1+r}\left(\frac{\sigma}{\sigma_y}\right)^r\right\} \qquad (3)$$

where, ε = strain, σ_y = the yield stress, and α and r are dimensionless parameters.

Substituting Equation(1) into (3) we get the strain at x;

$$\varepsilon = \frac{\sigma_{max} - \frac{\tau}{A}x}{E}\left\{1 + \frac{\alpha}{1+r}\left(\frac{\sigma_{max} - \frac{\tau}{A}x}{\sigma_y}\right)^r\right\} \qquad (4)$$

The elongation, δ, is obtained by integrating the strain given by Equation (4) from 0 to l with respect to x, as follows;

$$\delta = \int_0^l \varepsilon \, dx$$

$$= \frac{l}{E}\left(\sigma_{max} - \frac{\tau}{2A}l\right) - \frac{\alpha A}{E(1+r)(2+r)\tau\sigma_y^r}$$

$$\cdot\left\{\left(\sigma_{max} - \frac{\tau}{A}l\right)^{r+2} - \sigma_{max}^{r+2}\right\} \qquad (5)$$

By assuming that the pipelines were deformed in accordance with the ground displacements, the magnitude of elongation at l = 75 m was estimated to be 0.0561 m.

3.2 Stress-strain relationships in the pipes

It is necessary to determine the parameters α and r for the analyzed pipes, Grade-B and X-52 steels. The stress-strain curves shown in Figure 5 were used for these pipes. The parameters were α = 10 and r = 100 for the Grade-B steel and α = 9 and r = 10 for the X-52 steel.

The yield stresses of the Grade-B and the X-52 steels are 228 Mpa (2320 kg/cm2, 33 ksi) and 359 Mpa (3660 kg/cm2, 52 ksi), respectively. After yielding, the Grade-B steel has a very flat slope, but the X-52 steel has a steep slope.

3.3 Results

The length, l, was 75 m and the elongation, δ, was 0.0561 m. The depth of the pipes, H, was determined from Table 1, and the unit weight of soil was assumed to be 1.8 g/cm3. For the parameters Ko and ϕ, the values of 0.5, 0.75, 1.0 and 30°, 35°, 40° were assumed.

The maximum tensile stresses normalized by the yield stress, σ_{max}/σ_y obtained from Equation (6) are shown in Figure 6. This figure shows that the stress ratios for the Grade-B steel are almost 1, but much smaller than 1 for the X-52 steel. This means that these stresses are nominally sufficient to yield the Grade-B steel but not the X-52 steel. If the Grade-B steel in pipeline 8 had a relatively flat slope in the post yield portion of its stress-strain curve, as shown in Figure 5, then such stress would be sufficient to rupture the line. In contrast, the X-52 steel in pipelines 6a, 6b, 7 and 9 had both sufficient reserve against yield and ductility to sustain the ground deformation imposed on them. This means that the post-yield slope in the stress-strain curve, as well as the magnitude of the yield stress is very important, when a buried pipeline is subjected to large ground deformation.

4 CONCLUSIONS

The 1971 San Fernando earthquake provides the opportunity to relate large ground deformation, various soil conditions, and the response of buried pipelines of different size, composition, and age. Of particular interest is the area west of the Upper Van Norman Reservoir, where liquefaction-induced soil movements subjected six different pipelines to virtually the same pattern of gro-

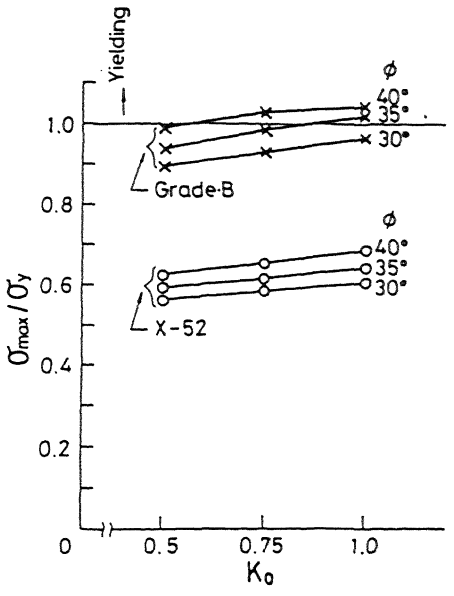

Figure 6. The normalized maximum stresses induced in the analyzed pipes.

und displacement.

A reliable record of pipeline performance involves both failed pipelines and those which were able to sustain large differential movement. In order to understand this phenomena, numerical analyses were performed.

The results revealed that the stresses induced in the pipelines were nominally sufficient to yield the Grade-B steel, but not the X-52 steel. Steels with relatively low yield stress, particularly those manufactured over 20 to 30 years ago, such as the Grade-B steel, may be characterized by a relatively flat slope when tensile stress is plotted with respect to strain in the post yield range of axial deformation. In contrast, high stress steels with steeper post-yield slopes, such as the X-52 steel are able to accommodate ground movement even though the magnitude maybe several meters. This shows that the post-yield slope is critically important for the level of maximum strain in the steel as well as the yield stress when a buried pipeline is subjected to tensile ground movements.

REFERENCES

Hamada, M., S. Yasuda, R. Isoyama, and K. Emoto 1985. Study of liquefaction-induced permanent ground displacements. Association for the Development of Earthquake Prediction, Tokyo.

O'Rourke, T.D., B.L. Roth, & M. Hamada 1989. A case study of large ground deformation during the 1971 San Fernando earthquake. 2nd U.S.-Japan workshop on liquefaction, large ground deformation, and their effects on lifeline facilities. 67-81.

O'Rourke, T.D. & M.S. Tawfik 1983. Effects of lateral spreading on buried pipelines during the 1971 San Fernando earthquake. PVP-Vol.77, ASME. New York. 124-132.

O'Rourke, T.D., B.L. Roth, F. Miura, and M. Hamada 1990. Case history of high pressure pipeline response to liquefaction-induced ground movements. Proc. of Fourth U.S. National Conf. on Earthquake Eng. Palm Springs. 955-964.